SAND2014-1158C

Power-Penalty Comparison of Push-Pull and Traveling-Wave Electrode Silicon Mach–Zehnder Modulators

T. Latchu, M. Pochet, N. G. Usechak[1], C. DeRose[2], A. Lentine[2], D. C. Trotter[2], M. R. Watts[2], and W. Zortman[2]

US Air Force Institute of Technology, 2950 Hobson Way, WPAFB, Ohio 45433 (michael.pochet@afit.edu)
[1]US Air Force Research Laboratory, 2241 Avionics Circle, WPAFB, OH 45433
[2]Sandia National Labs, P. O. Box 5800, Albuquerque, NM 87185

Abstract: Power-penalty measurements on two Si Mach–Zehnder modulator designs, each compatible with standard CMOS processing, were performed. The results highlight the power penalty and bandwidth advantages of the traveling-wave electrode design over a push-pull single-electrode design.

OCIS Codes: (130.3120) Integrated optical devices; (060.4510) Optical communications

1. Introduction

Low-power, high-speed, small-footprint optical modulators capable of CMOS integration have been the focus of a vast amount of research over the past decade [1]. In this work, two Mach–Zehnder Modulator (MZM) designs fabricated using CMOS-compatible processing steps are characterized with respect to one another. The first topology uses electrodes designed according to a lumped-element model but with a series push-pull (PP) modulation scheme, while the second uses a segmented traveling-wave (TW) electrode design with a single-arm modulation scheme. The TW electrode design, where the propagation of the electrical signal is matched to that of the optical wave, yielded an increased bandwidth and a significant power-penalty improvement over the single-drive PP design.

2. Modulation Results

The three devices tested in this work are shown in Fig. 1. From top to bottom in Fig. 1 are 1000- and 2000-μm long PP MZMs, followed by a TW electrode device with an effective active region length of 1500 μm. The three MZM devices under test were fabricated at Sandia National Labs; device design and fabrication details can be found in [2, 3]. The electrode design and modulation scheme all have implications for the required drive voltage, device bandwidth, and extinction ratio (ER) – the expectation being that the PP MZMs will have a smaller bandwidth, while the matched electrical and optical propagation through the TW MZM is expected to yield a higher bandwidth. For the TW case, however, the impact on power penalty is not certain and is therefore the focus of this work.

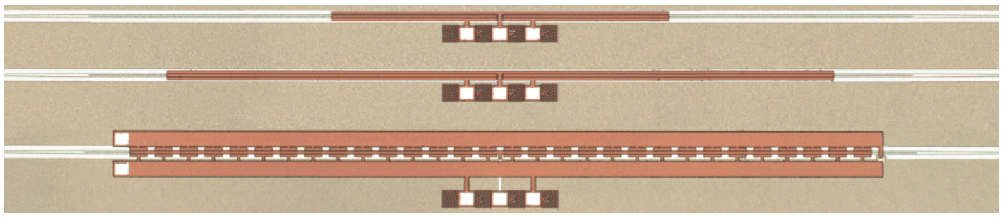

Fig. 1. The three MZMs under test; from top to bottom the 1000-μm Push-Pull MZM, the 2000-μm Push-Pull MZM, and the 1500-μm segmented TW electrode MZM with a built-in 50Ω termination on the TWE. The TW device is self terminated with an n^+ resistor (far right of device).

Characterization of the devices used a fiber-coupled Tunable Laser to seed a fiber amplifier to improve the overall signal-to-noise ratio of the measurements. A lensed fiber coupled light into and out of the MZMs, with the TE mode of the optical input aligned with the principal axes of the silicon waveguide via a fiber polarization controller. The optical output of the MZM was amplified using a second optical amplifier, whose output was sent to a variable optical attenuator (VOA) followed by a 99:1 fiber splitter. A 50-GHz high-speed photodetector with a high damage threshold was used to convert the output to an electrical signal which was directly connected to a Tektronix BSA286C BERTScope. Any required DC bias voltages were applied using the GSG pads and a Krohn-Hite Precision DC source. The RF and DC signals were both applied to the GSG pads by way of a bias tee for the PP MZMs, while the RF signal was applied separately to the GS pads on the TW MZMs; these pads are pictured on the left of the bottom device in Fig. 1.

DC characterization was conducted to determine the optimal bias voltage and driving voltage for the PP MZMs, as well as the static ER. These experiments were performed from 1540 to 1583 nm with bias voltages ranging from −10 to 10 V, while measuring transmission. The nature of the TW device does not provide equivalence between bias voltage characterization and expected performance at RF speeds, unlike the PP device, as the TW device has bias

and RF signals applied via two separate sets of pads. For the 1000-µm PP device, the mean V_π was 9.31 V with a standard deviation of 0.37 V, and for the 2000-µm PP device, the mean V_π was 3.77 V with a standard deviation of 0.08 V. These values produce a mean static extinction ratio (ER) of 18.57 dB and 10.90 dB with standard deviations of 0.72 dB and 2.83 dB, respectively. The RF experimental setup was limited to driving voltages of ≤ 2 V_{pp}, which decreases the expected ER. After selecting the optimum bias voltages of −4.3 V for the 1000-µm PP MZM and −2.6 V for the 2000-µm PP MZM, the expected static ERs were reduced to 5.11 dB and 5.27 dB, respectively. For reference, the TW MZM was biased at 4 V, which, due to device design, operates the device in its depletion mode. The thorough DC characterization facilitates optimal biasing conditions during RF characterization.

The power-penalty measurements for the three devices operated at 10 Gbps using the previously specified bias voltages, and a driving voltage of 2 V_{pp}, are given in Fig. 2(a). A 4.85-dB power penalty between the 1500-µm TW and 1000-µm PP MZMs, and a 3.68-dB power penalty between the 1500-µm TW and 2000-µm PP MZMs was measured. The received optical power was decreased using the VOA; this increases the OSNR, and therefore results in an increase in BER. Eye diagrams for each of the MZMs are shown in Figure 2(b-c), where 10-Gbps error-free operation was observed in each given appropriate delay and threshold conditions. As can be seen in the figure, the static ER is not the optimal indicator in device performance when the devices are operated at high speed. Instead, the eyes on the PP devices are minimally open due to bandwidth limitations, despite the fact that PP MZMs would be expected to display a higher ER for a given drive voltage. Maximum error-free bit rates of 13, 11.25, and 16 Gbps were measured for the 1000- and 2000-µm PP and 1500-µm TW electrode devices, respectively.

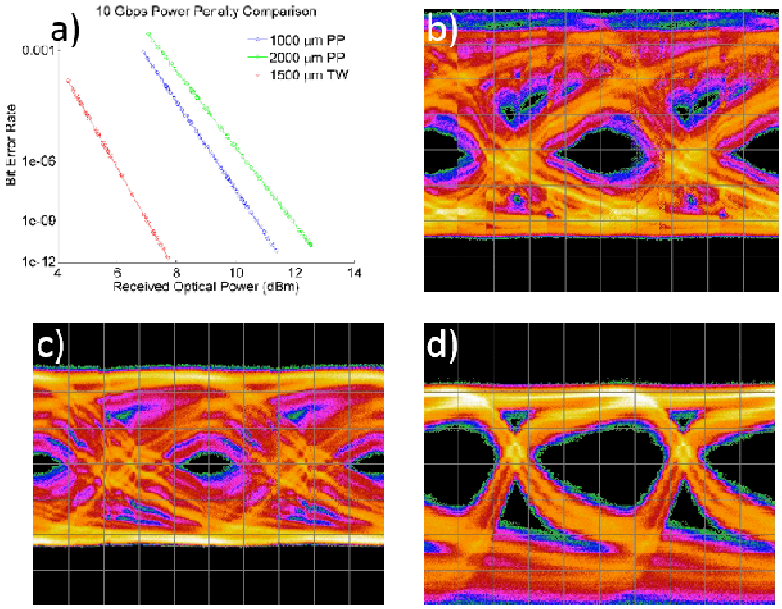

Fig. 2. (a) Comparison of the power penalty for all three devices when operating at a speed of 10 Gbps; (b) – (c) Eye diagrams for the three MZMs at 10 Gbps, with all MZMs in error-free operation; (b) 1000-µm PP with an eye opening of 60.5 mV; (c) 2000-µm PP with an eye opening of 30.2 mV; (d) 1500-µm TW with an eye opening of 74.9 mV. For all cases, the modulators' input optical power was held constant.

3. Conclusions

The PP modulation scheme requires lower drive voltages than the TW device to achieve a given ER; however, the electrode design of this family of devices limits bandwidth, and when operating at high speeds, amplitude noise and timing jitter contribute significantly to eye closure. As the TW device has a larger bandwidth, it can operate at the same speed, while using the same driving voltage, as the PP device, and achieve a similar ER.

4. Acknowledgment

The views expressed in this article (88ABWXXXX) are those of the author & do not reflect the official policy or position of the U.S. Air Force, Department of Defense, or the U.S. Government. The work of N. Usechak & M. Pochet was supported through an AFOSR grant (12RY09COR). Sandia National Laboratories is a multi-program lab managed and operated by Sandia Corp., a wholly owned subsidiary of Lockheed Martin Corporation, for the U.S. Department of Energy's National Nuclear Security Administration under contract DE-AC04-94AL85000.

5. References

[1] X. Xiao, H. Xu, X. Li, Z. Li, T. Chu, Y. Yu, and J. Yu, Optics Express 21(4), 4116-4125 (2013).
[2] C. T. DeRose, D. C. Trotter, W. A. Zortman, and M. R. Watts, *Optical Interconnects Conference*, vol. 6, 135–136 (2012).
[3] M. R. Watts, W. A. Zortman, D. C. Trotter, R. W. Young, and A. L. Lentine, *IEEE J. Sel. Top. Quantum Electron.* 16(1), 159–164 (2010).